Asymptotic stability of contraction-driven cell motion

C. Alex Safsten,[1] Volodmyr Rybalko,[2] and Leonid Berlyand[3,*]
[1]*Department of Mathematics, The Pennsylvania State University, Pennsylvania, USA*
[2]*B. Verkin Institute for Low Temperature Physics and Engineering, Kharkiv, Ukraine*
[3]*Department of Mathematics and Huck Institute for Life Sciences, The Pennsylvania State University, Pennsylvania, USA*

(Received 19 July 2021; accepted 24 December 2021; published 14 February 2022)

We study the onset of motion of a living cell (e.g., a keratocyte) driven by myosin contraction with focus on a transition from unstable radial stationary states to stable asymmetric moving states. We introduce a two-dimensional free-boundary model that generalizes a previous one-dimensional model [P. Recho, T. Putelat, and L. Truskinovsky, Phys. Rev. Lett. **111**, 108102 (2013)] by combining a Keller-Segel model, a Hele-Shaw boundary condition, and the Young-Laplace law with a regularizing term which precludes blowup or collapse by ensuring that membrane-cortex interaction is sufficiently strong. We find a family of asymmetric traveling solutions bifurcating from stationary solutions. Our main result is nonlinear asymptotic stability of traveling solutions that model observable steady cell motion. We derive an explicit asymptotic formula for the stability-determining eigenvalue via asymptotic expansions in small speed. This formula greatly simplifies computation of this eigenvalue and shows that stability is determined by the change in total myosin mass when stationary solutions bifurcate to traveling solutions. Our spectral analysis reveals the physical mechanisms of stability.

DOI: 10.1103/PhysRevE.105.024403

I. INTRODUCTION

Sustained motion on a substrate has been observed in experiments on living cells, e.g., keratocytes. They are found naturally moving on flat surfaces, e.g., the human cornea, making them ideal subjects for experiment. Moreover, their flat shape lends itself to two-dimensional (2D) modeling. Keratocytes are often observed in a stationary state with a circular shape, or traveling with constant velocity and maintaining a constant, asymmetric shape. This motion is explained by three mechanisms: adhesion, protrusion, and contraction, the effects of which are summarized as follows. The cytoskeleton which provides structure for the cell plays a key role in this motion and it contains actin and myosin proteins. Actin polymerizing near the edge of the cell causes protrusions of the cell membrane. These protrusions then adhere to the substrate, stabilizing the cell in its new shape. Myosin causes the actin polymers to contract. If the myosin is concentrated on one side of the cell, the cell contracts on that side, driving intracellular fluid to the other side of the cell and expanding the cell on that side. The flow of intracellular fluid also carries the myosin to the other side of the cell, continuing the process and resulting in net motion. The study of cytoskeleton gel has led to the recent development of the so-called active gel physics [1].

We introduce a 2D free-boundary partial differential equation model for cell motility which describes the evolution of the cell shape and the distribution of myosin within the cell. In [2], it is argued that at least some cells are driven exclusively by myosin contraction (as opposed to adhesion or protrusion), and our model supports this claim by showing steady motion resulting from myosin contraction only. This model exhibits bifurcation of a family of traveling solutions (modeling cells moving with constant velocity and shape) from a family of stationary solutions (modeling nonmoving cells).

In order to be observed in experiment, steady cell motion must be robust, not disrupted by small perturbations present in any experimental setup. This property can be established theoretically by proving *asymptotic stability* of traveling solutions; that is, solutions that start close to a traveling solution not only stay close, but eventually converge to this traveling solution (and we introduce a proper notion of convergence for traveling solutions). We show that traveling solutions to our model have this property by showing that they are asymptotically stable. Stability is also important for numerical computations. Since any computational model of a moving cell is necessarily an approximation of a true cell, stability of traveling solutions is necessary for numerical simulations of cell motion to converge.

A one-dimensional (1D) contraction-driven free-boundary model is proposed in [2,3] (see more recent work [4]). Our model generalizes this to one to two dimensions, and establishes conditions for the stability of traveling solutions. We show that asymmetry in the myosin distribution results in the net motion of the cell, c.f. "motor effect" [5].

A 2D free-boundary model for cell motion driven by polymerization of actin (as opposed to myosin contraction) is proposed in [6]. Like our model, this model also possesses a branch of traveling solutions bifurcating from a family of stationary solutions. Analysis shows that the bifurcation in this model is subcritical, meaning that traveling solutions near the bifurcation point are unstable (see also a 2D model in [7]). Our main objective is to go beyond linearized stability and establish analytically the nonlinear stability of steady cell motion

*lvb2@psu.edu

described by traveling solutions for a wide range of physical parameters (c.f. numerics for linearized stability, e.g., [6,8]). This is done by deriving a simple *explicit asymptotic formula* for the stability determining eigenvalue in two dimensions. The derivation of this formula is based on a special ansatz for the corresponding eigenvector with interesting asymptotic behavior due to the non-self-adjoint nature of the problem, a key mathematical feature of living systems. For technical simplicity, derivation of nonlinear stability from linearity is done in the 1D setting (via asymptotics for semigroups; see Supplemental Material [9]), but we do not use any specific 1D argument and our techniques apply in the 2D model.

Other 2D free-boundary models of cell motility have been examined numerically, e.g., [6,10,11]. For example, in [10], the authors propose a model for keratocyte motility taking into account actin polymerization in addition to myosin-driven contraction. Numerical analysis of this free-boundary model shows close agreement with both experimental results and theoretical results in our model. Additionally, a 2D moving cell model where the boundary has fixed shape was introduced and studied analytically and numerically in [12]. This model possesses several stationary solutions the stability of which is proved provided the total myosin mass is sufficiently small.

Phase-field models of cell motion provide an alternative to free-boundary models. Computational results of these models, shown in, e.g., [13,14], also agree qualitatively with results from our free-boundary model.

II. THE MODEL

Consider a 2D model for a cell occupying a region $\Omega(t)$ with free boundary. Following [6,11,15], we study a friction-dominated regime so the flow of acto-myosin gel satisfies Darcy's law: $\nabla\sigma = \zeta u$, σ is the scalar stress (pressure), u is the velocity, and ζ is the constant adhesion coefficient. Generalizing the 1D constitutive equation from [2], the 2D constitutive equation is $\sigma = \mu\,\mathrm{div} u + km$. Here, μ, m, and k are the constant bulk viscosity of the gel, myosin density, and constant contractility coefficient which models a steady supply of energy (from, e.g., adenosine triphosphate) so that the myosin creates a constant active contractile stress per motor. This constitutive equation is obtained by substituting Darcy's law into the force-balance equations used in [1,10] while using the fact that for acto-myosin gel bulk viscosity dominates shear viscosity (p. 3 in Supplemental Material of [10]; see also [16]). For simplicity, we choose $\mu = k = 1$.

On the boundary $\partial\Omega$ with curvature κ the Young-Laplace law $\sigma = p_h + p_e - \gamma\kappa$ holds, $\gamma > 0$ is the constant surface tension coefficient, p_h is the constant hydrostatic pressure, and p_e is the elastic restoring force due to membrane cortex tension. Following the 1D model [2–4], p_e is nonlocal (c.f., vertex models [17]) and given by

$$p_e(|\Omega|) = -k_e\frac{|\Omega| - |\Omega_h|}{|\Omega_h|}, \tag{1}$$

where k_e is the constant *inverse compressibility coefficient* and $|\Omega_h|$ is a reference area, i.e., the typical area occupied by a cell at rest.

Myosin density obeys the advection-diffusion equation $\partial_t m = \Delta m - \mathrm{div}(um)$ with the no-flux condition $\partial_\nu m = 0$ on $\partial\Omega(t)$ [ν normal to $\partial\Omega(t)$]. The free boundary moves according to the kinematic condition $V_\nu = \partial_\nu\sigma/\zeta$.

We study the following free-boundary problem obtained from the above equations by introducing the auxiliary potential $\phi = \sigma/\zeta$ and $p_* = p_h + p_e$:

$$0 = \Delta\phi + m - \zeta\phi \quad \text{in } \Omega(t), \tag{2}$$

$$\partial_t m = \Delta m - \mathrm{div}(m\nabla\phi) \quad \text{in } \Omega(t), \tag{3}$$

$$\zeta\phi = p_*(|\Omega(t)|) - \gamma\kappa \quad \text{on } \partial\Omega(t), \tag{4}$$

$$\partial_\nu m = 0 \quad \text{on } \partial\Omega(t), \tag{5}$$

$$V_\nu = \partial_\nu\phi \quad \text{on } \partial\Omega(t). \tag{6}$$

Among the solutions to (2)–(6) is the following family of simple, constant, stationary solutions (verified by direct substitution), which will be used in our bifurcation analysis: $m_0 = p_*(\pi R^2) - \gamma/R$, $\phi_0 = m_0/\zeta$, and $\Omega_0(t)$ a disk of radius R.

Hereafter we assume the following condition holds:

$$k_e > \left(m_0 + \frac{\gamma}{2R}\right)\frac{|\Omega_h|}{\pi R^2}. \tag{7}$$

This condition eliminates mathematical artifacts such as a cell collapsing to a point for small k_e. It ensures that membrane cortex tension is sufficiently strong to balance the contractive effects of myosin and surface tension. Differentiation in R shows that (7) implies that the total myosin mass

$$M(R) = \pi R^2 m_0 = p_*(\pi R^2)\pi R^2 - \pi\gamma R \tag{8}$$

decreases strictly (parametrizations by R or M are interchangeable).

III. BIFURCATION OF TRAVELING SOLUTIONS

Substituting the ansatz $\phi = \phi(\mathbf{x} - \mathbf{V}t)$, $m = m(\mathbf{x} - \mathbf{V}t)$, $\Omega = \Omega_0 + \mathbf{V}t$ for the traveling solutions with velocity $\mathbf{V} \in \mathbb{R}^2$ into (2)–(6), we find that (2), (4), and (5) are unchanged while (3) and (6) become

$$\partial_t m = \mathbf{V}\cdot\nabla m + \Delta m - \mathrm{div}(m\nabla\phi), \tag{9}$$

$$0 = \partial_\nu(\phi - \mathbf{V}\cdot\mathbf{x}), \tag{10}$$

respectively. Substituting into (9) solutions of the form $m = \Lambda(\mathbf{V})e^{\phi - \mathbf{V}\cdot\mathbf{x}}$, we reduce (2)–(6):

$$0 = \Delta\phi + \Lambda e^{\phi - \mathbf{V}\cdot\mathbf{x}} - \zeta\phi \quad \text{in } \Omega, \tag{11}$$

$$\zeta\phi = p_*(|\Omega|) - \gamma\kappa \quad \text{on } \partial\Omega, \tag{12}$$

$$0 = \partial_\nu(\phi - \mathbf{V}\cdot\mathbf{x}) \quad \text{on } \partial\Omega \tag{13}$$

for unknowns $\phi(\mathbf{x}, \mathbf{V})$, $\Omega(\mathbf{V})$, and $\Lambda(\mathbf{V})$. When $\mathbf{V} = 0$, we recover the stationary solution ϕ_0, m_0, and Ω_0. We write the cell boundary $\partial\Omega$ in polar coordinates $R + \rho(\theta, \mathbf{V})$ [where $\rho(\theta, 0) = 0$] chosen such that $\theta = 0$ is the direction of $\mathbf{V}$. Then ϕ, ρ, and Λ depend only on $V = |\mathbf{V}|$. To find total

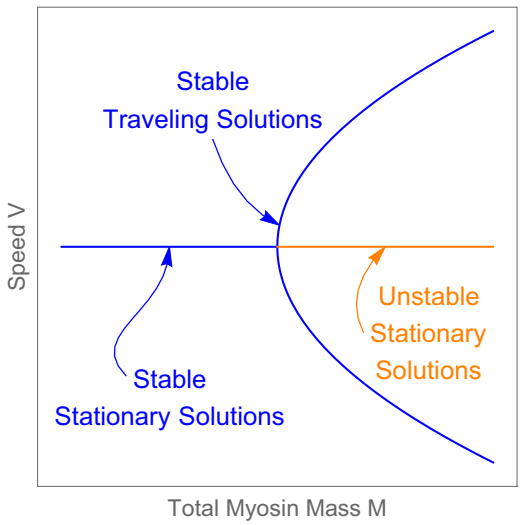

FIG. 1. Supercritical bifurcation diagram ($M_2 > 0$). For subcritical bifurcation, see Supplemental Material [9].

myosin mass $M(V)$ we expand solutions (ϕ, ρ, Λ) for small V:

$$\phi(r,\theta,V) = \sum_{i=0}^{3} \phi_i(r,\theta)V^i + O(V^4), \tag{14}$$

$$\rho(\theta,V) = \rho_1(\theta)V + \rho_2(\theta)V^2 + \rho_3(\theta)V^3 + O(V^4), \tag{15}$$

$$\Lambda(V) = \Lambda_0 + \Lambda_1 V + \Lambda_2 V^2 + \Lambda_3 V^3 + O(V^4). \tag{16}$$

Substituting the expansions (14)–(16) into (11)–(13), we obtain coefficients ϕ_n, ρ_n, and Λ_n iteratively. In (12) and (13) we expand ϕ about $r = R$ to transform the boundary conditions on the unknown $\partial\Omega$ to a fixed boundary $r = R$. Then ϕ_1 is the product of an explicitly known function of r and $\cos\theta$, $\rho_1 = \Lambda_1 = 0$.[1] For $n \geqslant 2$, ϕ_n is the sum of Fourier modes $\cos(k\theta)$, $k \leqslant n$, and Fourier coefficients are found numerically (see Supplemental Material [9]).

The parameters R, ζ, γ, k_e, and p_h are chosen so that ϕ_1 satisfies (12) and (13) [c.f. when $n \geqslant 2$, ρ_n and Λ_n are chosen so ϕ_n satisfies (12) and (13)], leading to a transcendental equation for the critical radius $R_0 = R_0(\zeta, \gamma, k_e, p_h)$ of stationary solutions when they bifurcate to traveling solutions:

$$F(R,\zeta,\gamma,k_e,p_h) := \frac{\zeta I_1(Rs)}{s^3 I_1'(Rs)} - \frac{(\zeta - s^2)R}{s^2} = 0, \tag{17}$$

where $s = \sqrt{\zeta - p_*(\pi R^2) + \gamma/R}$, and I_1 is the modified Bessel function.

The stationary and traveling solutions are parametrized by M and V, respectively. The bifurcation occurs at $M = M_0$ obtained by substituting R_0 in (8) (see Fig. 1). The total myosin

[1]No uniqueness for system (2)–(6): if $\phi(\mathbf{x},t)$, $m(\mathbf{x},t)$, and $\Omega(t)$ solve (2)–(6), so does the translation $\phi(\mathbf{x}-\mathbf{y},t)$, $m(\mathbf{x}-\mathbf{y},t)$, and $\Omega(t)+\mathbf{y}$. Taking $\rho_1 = 0$ we select the traveling solution centered at the origin, $\Lambda_1 = 0$, since $\Lambda(V) = \Lambda(-V)$.

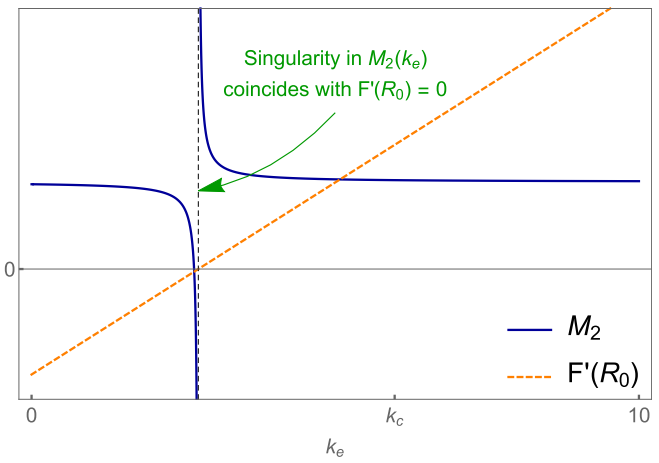

FIG. 2. The dependence of M_2 on k_e. Note $M_2 > 0$ when $k_e > k_c$, i.e., when (7) is satisfied. See Supplemental Material [9] for parameter values used for simulations.

mass of traveling solutions is

$$M(V) = \int_0^{2\pi}\int_0^{R_0+\rho} \Lambda(V) e^{\phi(r,\theta,V)-Vr\cos\theta} r\,dr\,d\theta \tag{18}$$

$$= M_0 + M_1 V + M_2 V^2 + O(V^4), \quad M_0 = m_0\pi R_0^2, \tag{19}$$

$$M_1 = 0,\ M_2 = 2\pi\zeta \int_0^{2\pi} \frac{m_0 R_0^2}{\gamma - 2k_e R_0}\phi_2(R_0,\theta)\,d\theta + \int_0^{2\pi}\int_0^{R_0} \phi_2(r,\theta) r\,dr\,d\theta. \tag{20}$$

In Sec. IV, it will be shown that the sign of M_2 determines the stability of traveling solutions, and this sign depends on R_0, m_0, ζ, γ, and k_e. Figure 2 shows the key dependence of M_2 on k_e. Note that M_2 has a singularity at $k_e = k_*$—for this value of k_e, the bifurcation is not smooth. Numerically, for most parameter values, $M_2 > 0$. Also, $M_2 > 0$ for all $k_e > k_c$, the minimal value of k_c where (7) holds.

Next, we solve for the coefficients ρ_n of the curve $r = R + \rho(\theta, V)$ that determines the boundary $\partial\Omega$ of traveling solutions. Then $\rho_1 = 0$, while $\rho_2(\theta) = a + b\cos(2\theta)$ and $\rho_3(\theta) = c\cos(3\theta)$, where a, b, and c depend on ϕ_2, ϕ_3 (both found numerically), and physical parameters. Figure 3 shows the evolution of cell shape and myosin density. It qualitatively agrees with simulations from a similar free-boundary model (see Fig. 1 in [18]) and a phase-field model (see Fig. 3 in [13]).

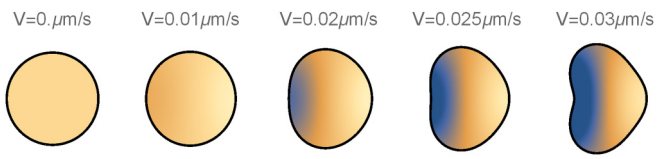

FIG. 3. Simulations for the cell shape and myosin density as speed increases. Motion is to the right. Darker colors indicate higher myosin density. See Supplemental Material [9] for parameter values used for simulations.

IV. STABILITY OF TRAVELING SOLUTIONS

Observable steady motion of the cell corresponds to *stable* traveling solutions. However, the standard notion of Lyapunov stability needs to be *generalized to traveling solutions*. Namely, the best one can hope for is *stability up to shifts, rotations, and velocity changes*, understood as follows. Denote a traveling solution to (2)–(6) with velocity $\mathbf{V}$ as $u_0(t,\mathbf{V}) := (m_0(\mathbf{x},t,\mathbf{V}),\Omega_0(t,\mathbf{V}))$. Consider another traveling solution $u_1(t,\mathbf{V})$, obtained by an $\varepsilon \ll 1$ shift of u_0 in the x direction. Asymptotic stability implies that a small perturbation $\tilde{u}$ close to both u_0 and u_1 at $t=0$ is exponentially close to only one of them at $t=T\gg 1$. Thus, solutions that are shifts of one another should not be distinguished. Even more dramatic changes in stability occur if at $t=0$ we consider $u_0(t,\mathbf{V}_0)$ and $u_1(t,\mathbf{V}_1)$ such that $\mathbf{V}_0-\mathbf{V}_1=\vec{\delta}$, $0<|\vec{\delta}|\ll 1$. Then at $t=T\gg 1$, these solutions will be a *large distance* $|\vec{\delta}|T$ apart, and a small perturbation $\tilde{u}$ of u_0 and u_1 at $t=0$ will be far away from either u_0 or u_1 at $t=T$. Again, stability does not hold in the classical sense and one should not distinguish solutions obtained by rotations (changes direction of velocity) and finite shifts of one another (solutions are observed in translated or rotated coordinates).

Initial perturbations at $t=t_0$ are *arbitrary*; therefore, at $t>0$, $u(t,\mathbf{V})$ may not be a traveling solution. However, due to asymptotic stability, it becomes such a solution as $t\to\infty$ with the same myosin mass M as at $t=0$, which uniquely determines speed $|\mathbf{V}|$ (conservation of M).

To show that stability is determined by a special eigenvalue, rewrite (2)–(6) in a phase space (m,ρ):

$$\frac{\partial}{\partial t}(m,\rho)=F(m,\rho). \tag{21}$$

Here F is a nonlinear operator from (2)–(6), and ϕ is an auxiliary function determined by (2) and (4). Introduce the linearizations $A_S(R)$ and $A_T(\mathbf{V})$ of F about the stationary and traveling solutions, respectively, ($A_T(\mathbf{V})$ is found in coordinates moving with velocity $\mathbf{V}$ so the traveling solution appears stationary). At the bifurcation point, the families of traveling and stationary solutions intersect: $A_S(R_0)=A_T(0)$. The signs of the real parts of the eigenvalues of $A_S(R)$ and $A_T(\mathbf{V})$ determine the stability of the stationary and traveling solutions. For $R\neq R_0$, all the eigenvalues of $A_S(R)$ are negative except the zero eigenvalue (multiplicity 3) and an eigenvalue $E(R)$ (multiplicity 2) the sign of which is determined by (24) since $E(R_0)=0$. Similarly, for $\mathbf{V}\neq 0$, all eigenvalues of $A_T(\mathbf{V})$ are negative except the zero eigenvalue (multiplicity 4), and an eigenvalue $\lambda(V)$ (multiplicity 1) the sign of which *determines stability of traveling solutions*.

Away from the bifurcation point, each of the eigenvectors of $A_S(R)$ [or $A_T(\mathbf{V})$] corresponding to the zero eigenvalue is a derivative of the stationary (or traveling) solution in a parameter, e.g., the coordinates of the center of mass with respect to which the class of stationary (or traveling) solutions is invariant. Both $A_S(R)$ and $A_T(\mathbf{V})$ have two eigenvectors $\mathcal{E}_x$ and $\mathcal{E}_y$ for the zero eigenvalue corresponding to invariance with respect to shifts in the x and y directions. Additionally, $A_S(R)$ has another eigenvector corresponding to invariance with respect to a change in the radius R. For the zero eigenvalue, $A_T(\mathbf{V})$ also has two *generalized* eigenvectors corresponding to infinitesimal changes in speed and direction of motion (rotation) of traveling solutions. Consider, for instance, the vector $b(\mathbf{V})=\frac{\partial}{\partial V}u_0(t,\mathbf{V})$ in $V=|\mathbf{V}|$ (change in speed). Then $A_T(\mathbf{V})b(\mathbf{V})=a(\mathbf{V})$ where $a(\mathbf{V})=(\mathcal{E}_x\mathbf{V}\cdot e_x+\mathcal{E}_y\mathbf{V}\cdot e_y)/|\mathbf{V}|$ is the eigenvector of $A_T(\mathbf{V})$ for the zero eigenvalue corresponding to invariance with respect to shifts in the direction of motion $\mathbf{V}/|\mathbf{V}|$. To see this, consider the traveling solution $u(t,\mathbf{V})$ to the nonlinear problem (21) with velocity $\mathbf{V}$ and perturb its velocity by $\mathbf{V}'=\mathbf{V}+\varepsilon\mathbf{V}/|\mathbf{V}|$ to obtain $u(t,\mathbf{V}')$, another traveling solution of (21). Substituting $u(t,\mathbf{V}')$ into the linearization of (21) about $u(t,\mathbf{V})$ and taking $t=0$ shows that $A_T(\mathbf{V})b(\mathbf{V})=a(\mathbf{V})$, that is, $b(\mathbf{V})$ is a generalized eigenvector.

The eigenvectors $a(\mathbf{V})$ and $b(\mathbf{V})$ play a key role in the ansatz (22) below, which is used in calculating the stability-deciding eigenvalue $\lambda(V)$. The eigenvector $c(\mathbf{V})$ corresponding to $\lambda(V)$ becomes parallel to $a(\mathbf{V})$ as $V\to 0$ (c.f. orthogonality of eigenvectors for self-adjoint operators) and $\lambda(V=0)=0$. The eigenvalue $\lambda(V)$ is even (due to symmetry $x\mapsto -x$, $V\mapsto -V$), thus $\lambda'(0)=0$ and $\lambda(V)=\lambda_2V^2+O(V^4)$. Therefore the stability is determined by the sign of λ_2.

Both $a(\mathbf{V})$ and $b(\mathbf{V})$ can be found explicitly as derivatives of traveling solutions with asymptotic expansions (14)–(16). To find λ_2, we introduce a special ansatz (see Supplemental Material [9]) for $c(\mathbf{V})$ starting with coefficients $a(\mathbf{V})$ and $b(\mathbf{V})$:

$$c(\mathbf{V})=a(\mathbf{V})+\lambda_2V^2b(\mathbf{V})+O(|\mathbf{V}|^3) \tag{22}$$

Substituting (22) into $A_T(\mathbf{V})c(\mathbf{V})=\lambda(\mathbf{V})c(\mathbf{V})$ and comparing terms of like power in V, we obtain λ_2, which requires solving equations up to fifth order in V (see [19] for details of this calculation); we obtain an *explicit formula*:

$$\lambda_2=-\frac{dE}{dM}\Big|_{M=M(0)}\frac{d^2M}{dV^2}\Big|_{V=0}. \tag{23}$$

Therefore, the stability of traveling solutions is determined by the signs of the two derivatives in (23). First, from (19), $\partial^2M/\partial V^2|_{V=0}=2M_2$ (see its sign in Fig. 2). In particular, $\partial^2M/\partial V^2|_{V=0}>0$ when condition (7) is met. Second, dE/dM is determined by F from (17):

$$\frac{dE}{dM}=\frac{dE}{dR}\frac{dR}{dM}=C\frac{\partial F}{\partial R}, \tag{24}$$

where $C>0$ (explicitly calculated in Lemma 4.5 in [19]). The eigenvalue $E(R)$ describes *moveability* of stationary solutions: if $\mathrm{Re}\,E(R)>0$, then stationary solutions "want to move," becoming motile after a small perturbation. Straightforward calculations show $E(R)=E(M)>0$ if $M>M_0$ and (7) holds [$E(R_0)=0$]. Figure 2 shows how $\partial F/\partial R|_{R=R_0}$ depends on k_e and $\partial F/\partial R|_{R=R_0}=0$ precisely when M_2 has a singularity. If condition (7) holds, then $\partial F/\partial R|_{R=R_0}$ and $\partial E/\partial M|_{M=M(0)}$ are both positive, so $\lambda_2<0$. All other eigenvalues of $A_T(\mathbf{V})$ have negative real part except the zero eigenvalue the eigenvectors of which correspond to shifts in the x and y directions, and generalized eigenvectors correspond to rotations, and shifts in speed (the latter controlled by conservation of myosin). Thus, for parameters satisfying (7), traveling solutions are *linearly stable* up to shifts and rotations.

This analysis explains the mathematics behind the stability of cell motility. Namely, instability of radial stationary states manifests itself in the presence of an eigenvector for the eigenvalue $E(R) > 0$ the structure of which is similar to eigenvector $c(V)$ in (22), corresponding to $\lambda(V)$. Indeed, the leading terms in both eigenvectors correspond to spatial shifts. The key difference is that $E(R) > 0$ while $\lambda(V) < 0$. Thus perturbations of stationary states lead to accelerating shift motion (translations) whereas perturbations of traveling solutions lead to a decelerating shift motion. Qualitatively, upon perturbation, an unstable stationary state starts to move and it eventually becomes a stable traveling solution.

V. NONLINEAR ASYMPTOTIC STABILITY: DISCUSSION AND RESULTS

Direct numerical computation of the eigenvalue $\lambda(V)$ the sign of which determines stability is quite difficult for several reasons. First, $\lambda(V)$ is small. Second, instability of numerical methods and computational error may become conflated with actual physical instability. Third, while numerical methods for self-adjoint problems based on variational principles are well developed, such principles are not available for non-self-adjoint problems that model out-of-equilibrium systems. However, we easily calculate $\lambda(V) = \lambda_2 V^2 + O(V^4)$ thanks to the explicit formula (23) for λ_2 in which dE/dM is explicitly found in (24) and it remains to compute d^2M/dV^2 via numerical evaluation of the integrals in (20).

These reasons highlight the importance of the analytical study of stability in our non-self-adjoint free-boundary model. Moreover, our analysis is not restricted to the linearized problem but establishes conditions for nonlinear stability. For example, multiple zero eigenvalues in the linearized problem with generalized eigenvectors lead to solutions that grow linearly as $t \to \infty$. Because of these eigenvalues, linearized stability analysis is inconclusive and we construct a Lyapunov function to establish nonlinear asymptotic stability when the parameters satisfy (7). This is done by proving that all eigenvalues except $\lambda(V)$ and zero eigenvalues have negative real part, while zero eigenvalues (and corresponding eigenvectors) are eliminated as follows. The shift or rotation eigenvectors are eliminated by mapping the free-boundary domain to a fixed domain such that if two vectors (m, ρ) differ only by a shift and rotation the governing equation (21) for them is the same, and the shift or rotation eigenvectors are mapped to zero because they are defined via differentiation in these shifts or rotations. Recall that V is uniquely determined by M and the conservation of M property [see the paragraph before (21)]. Thus the generalized eigenvector $b(\mathbf{V})$ corresponding to a change in speed is eliminated by considering solutions with fixed total myosin mass M in view of the conservation of M property. A possibility of a sequence of eigenvalues the negative real parts of which converge to zero is eliminated by *a priori* estimates presented in the Supplemental Material [9] in the 1D setting for technical simplicity. Finally, numerics for (23) determines that if $k_e > k_c$ [sufficiently strong membrane cortex elasticity; (7) holds] then asymptotic nonlinear stability follows. Note that our modeling and analysis are performed in the small velocity regime: $V \ll V_{\text{char}} = \zeta^{-1}(p_h/R)$. For larger velocities, the model needs to be modified, e.g., polymerization is no longer negligible.

VI. CONCLUSIONS

We proposed a 2D free-boundary model for cell motility the traveling solutions of which represent persistent motion of the cell. We first performed linear stability analysis of the traveling solutions. Linearizing about the traveling solution of velocity $\mathbf{V}$ resulted in two challenges: the linearized problem is not self-adjoint and it has zero eigenvalue of multiplicity 4 with both true and generalized eigenvectors corresponding to shifts in the x and y directions and to changes in speed and rotation angle of traveling solutions. This led us to introducing a *notion of generalized stability up to shifts or rotation and speed changes*, since the standard Lyapunov stability does not apply. Furthermore, we show that there is only one eigenvalue, $\lambda(V)$, which may have a positive real part. Moreover, the non-self-adjoint nature of the linearized problem manifests in the eigenvector $c(\mathbf{V})$ for $\lambda(V)$ becoming asymptotically parallel to one of the shift eigenvectors. This difficulty is resolved by a special ansatz for $c(\mathbf{V})$, employing a shift eigenvector and its corresponding generalized eigenvector as coefficients. This ansatz led to an *explicit asymptotic formula for* $\lambda(V)$ (in terms of physical quantities). Zero eigenvalues made the linear stability analysis inconclusive, requiring construction of a Lyapunov function for the generalized asymptotic stability of traveling solutions. We establish *nonlinear asymptotic stability* of traveling solutions by showing that $\lambda_2 < 0$ in (23) in a wide range of physical parameters (adhesion, surface tension, and total myosin mass).

Expansions (14)–(16) and (23) reveal the physical ingredients responsible for stability: the underlying force coupling and shape effects. Due to (23), stability is determined by M_2 in (19), which shows that the distribution of myosin is coupled with the shape [(33) and (34) in the Supplemental Material [9] couple M_2 and shape ρ_2; shape does not change in first order, $\rho_1 = 0$].

In summary, our analysis reveals the mathematical underpinnings of stability in the cell motility problem. The elastic regularization term introduced in our 2D model (2)–(6) by analogy with the 1D case [2] shows that sufficiently strong elastic constant k_e is necessary for the model to capture the motility phenomenon by avoiding mathematical instabilities such as collapse. We quantify what is meant by "sufficiently strong k_e" via (7). Our spectral analysis explains the mechanisms of the instability-stability transition. The explicit formula (23) shows that stability of traveling solutions is determined by the change in total myosin mass. Namely, if the total myosin mass exceeds the critical value $M(0) = M_0$ [$M''(0) > 0$ in (23)], then unstable stationary solutions become asymptotically stable traveling solutions. Finally, the comparison between eigenvectors corresponding to the stability deciding eigenvalues $\lambda(V)$ and $E(R)$ (end of Sec. IV) explains the mathematics behind the transition between stationary and moving states.

ACKNOWLEDGMENTS

We thank our colleagues I. Aronson, J. Casademunt, J.-F. Joanny, N. Meunier, A. Mogilner, J. Prost, R. Alert, and L. Truskinovsky for many useful discussions on our results and suggestions on the model. We also express our gratitude to the members of L. Berlyand's Pennsylvania State University (PSU) research team, R. Creese and M. Potomkin, for discussions. The work of L.B. and C.A.S. was partially supported by National Science Foundation Grant No. DMS-2005262. V.R. is grateful to PSU Center for Mathematics of Living and Mimetic Matter, and to PSU Center for Interdisciplinary Mathematics for support of his two stays at PSU. His travel was also supported by National Science Foundation Grants No. DMS-1405769 and No. DMS-2005262.

[1] J. Prost, F. Jülicher, and J.-F. Joanny, Active gel physics, Nat. Phys. **11**, 111 (2015).

[2] P. Recho, T. Putelat, and L. Truskinovsky, Contraction-Driven Cell Motility, Phys. Rev. Lett. **111**, 108102 (2013).

[3] P. Recho, T. Putelat, and L. Truskinovsky, Mechanics of motility initiation and motility arrest in crawling cells, J. Mech. Phys. Solids **84**, 469 (2015).

[4] T. Putelat, P. Recho, and L. Truskinovsky, Mechanical stress as a regulator of cell motility, Phys. Rev. E **97**, 012410 (2018).

[5] B. Perthame and P. E. Souganidis, Asymmetric potentials and motor effect: A homogenization approach, Ann. Inst. Henri Poincare C **26**, 2055 (2009).

[6] C. Blanch-Mercader and J. Casademunt, Spontaneous Motility of Actin Lamellar Fragments, Phys. Rev. Lett. **110**, 078102 (2013).

[7] L. Berlyand, J. Fuhrmann, and V. Rybalko, Bifurcation of traveling waves in a Keller-Segel type free boundary model of cell motility, Commun. Math. Sci. **16**, 735 (2018).

[8] P. Maiuri, J.-F. Rupprecht, S. Wieser, V. Ruprecht, O. Bénichou, N. Carpi, M. Coppey, S. de Beco, N. Gov, C.-P. Heisenberg, C. Lage, F. Lautenschlaeger, M. Le Berre, A.-M. Lennon-Duménil, M. Raab, H. R. Thiam, M. Piel, M. Sixt, and R. Voituriez, Actin flows mediate a universal coupling between cell speed and cell persistence, Cell **161**, 374 (2015).

[9] See Supplemental Material at http://link.aps.org/supplemental/10.1103/PhysRevE.105.024403 for See Secs. 1.1–1.3 for details of the calculation of asymptotic expansion coefficients. See Sec. 1.4 for parameter values used for simulations. See Sec. 1.5 for details of the subcritical bifurcation, including [21,22]. See Sec. 2 for details of the derivation of the ansatz (22). See Sec. 3 for details of the nonlinear stability analysis, including [20].

[10] E. Barnhart, K.-C. Lee, G. M. Allen, J. A. Theriot, and A. Mogilner, Balance between cell-substrate adhesion and myosin contraction determines the frequency of motility initiation in fish keratocytes, Proc. Natl. Acad. Sci. USA **112**, 5045 (2015).

[11] A. C. Callan-Jones, J.-F. Joanny, and J. Prost, Viscous-Fingering-Like Instability of Cell Fragments, Phys. Rev. Lett. **100**, 258106 (2008).

[12] C. Etchegaray, N. Meunier, and R. Voituriez, Analysis of a nonlocal and nonlinear Fokker-Planck model for cell crawling migration, SIAM J. Appl. Math. **77**, 2040 (2017).

[13] F. Ziebert and I. S. Aranson, Computational approaches to substrate-based cell motility, npj Comput. Mater. **2**, 16019 (2016).

[14] D. Shao, H. Levine, and W.-J. Rappel, Coupling actin flow, adhesion, and morphology in a computational cell motility model, Proc. Natl. Acad. Sci. USA **109**, 6851 (2012).

[15] M. A. Heinrich, R. Alert, A. E. Wolf, A. Kosmrlj, and D. J. Cohen, Self-assembly of tessellated tissue sheets by growth and collision, bioRxiv (2021).

[16] F. G. Schmidt, F. Ziemann, and E. Sackmann, Shear field mapping in actin networks by using magnetic tweezers, Eur. Biophys. J. **24**, 348 (1996).

[17] S. Alt, P. Ganguly, and G. Salbreux, Vertex models: from cell mechanics to tissue morphogenesis, Phil. Trans. R. Soc. B **372**, 20150520 (2017).

[18] K. Keren, Z. Pincus, G. M. Allen, E. L. Barnhart, G. Marriott, A. Mogilner, and J. A. Theriot, Mechanism of shape determination in motile cells, Nature (London) **453**, 475 (2008).

[19] V. Rybalko and L. Berlyand, Emergence of traveling waves and their stability in a free boundary model of cell motility, arXiv:2104.00491 (2021).

[20] K.-J. Engel and R. Nagel, *One-Parameter Semigroups for Linear Evolution Equations* (Springer, New York, 2000).

[21] M. Nickaeen, I. Novak, S. Pulford, A. Rumack, J. Brandon, B. Slepchenko, and A. Mogilner, A free-boundary model of a motile cell explains turning behavior, PLoS Comput. Biol. **13**, e1005862 (2017).

[22] C. I. Lacayo, Z. Pincus, M. M. VanDuijn, C. A. Wilson, D. A. Fletcher, F. B. Gertler, A. Mogilner, and J. A. Theriot, Emergence of large-scale cell morphology and movement from local actin filament growth dynamics, PLoS Biol. **5**, e233 (2007).